THE JOURNAL OF BIOLOGICAL CHEMISTRY VOL. 283, NO. 22, pp. 15072–15077, May 30, 2008
© 2008 by The American Society for Biochemistry and Molecular Biology, Inc. Printed in the U.S.A.

I_{SA} Channel Complexes Include Four Subunits Each of DPP6 and Kv4.2*

Received for publication, August 20, 2007 Published, JBC Papers in Press, March 25, 2008, DOI 10.1074/jbc.M706964200

Heun Soh[1] **and Steve A. N. Goldstein**[2]

From the Department of Pediatrics and Institute for Molecular Pediatric Sciences, Pritzker School of Medicine, Biological Sciences Division, University of Chicago, Chicago, Illinois 60637

Kv4 potassium channels produce rapidly inactivating currents that regulate excitability of muscles and nerves. To reconstitute the neuronal A-type current I_{SA}, Kv4 subunits assemble with DPP6, a single transmembrane domain accessory subunit. DPP6 alters function—accelerating activation, inactivation, and recovery from inactivation—and increases surface expression. We sought here to determine the stoichiometry of Kv4 and DPP6 in complexes using functional and biochemical methods. First, wild type channels formed from subunit monomers were compared with channels carrying subunits linked in tandem to enforce 4:4 and 4:2 assemblies (Kv4.2-DPP6 and Kv4.2-Kv4.2-DPP6). Next, channels were overexpressed and purified so that the molar ratio of subunits in complexes could be assessed by direct amino acid analysis. Both biophysical and biochemical methods indicate that I_{SA} channels carry four subunits each of Kv4.2 and DPP6.

Kv4 subunits are molecular components of the neuronal voltage-gated potassium current I_{SA} (1–3). Assemblies of these pore-forming subunits do not manifest the characteristics of native currents on their own. Rather, the single transmembrane accessory subunit dipeptidyl aminopeptidase 6 (DPP6)[3] is required to produce the appropriate surface expression and biophysical gating parameters (4). DPP10 is also found to associate with Kv4 subunits and yield similar effects (5–7). Potassium channel-interacting protein KChIP (8–12) may also be required with DPP6 and/or DPP10 to render native I_{SA} currents (6). Because DPP subunits are important to determine natural properties of these channels, we sought to establish the structural basis for their operation, specifically, their number in each channel complex.

Previously, we found cardiac I_{Ks} channels to be formed with two single transmembrane span MinK subunits and four KCNQ1 pore-forming subunits via functional assays (13, 14) and cardiac I_{to} channels to carry four soluble KChIP2 subunits and four Kv4 subunits using electron microscopy and direct amino acid analysis (15, 16). Here, the stoichiometry of channels naturally assembled with DPP6 and Kv4.2 subunits is first inferred through comparison of the activity of channels formed by Kv4.2 or linked Kv4.2-Kv4.2, Kv4.2-DPP6, or Kv4.2-Kv4.2-DPP6 pore-forming subunits with or without DPP6 and with or without KChIP2. Next, channels are formed with DPP6 and Kv4.2 carrying epitope tags to allow purification and determination of the molar ratio of subunits by direct amino acid analysis. Electrophysiological and biochemical interrogation reveals four DPP6 and four Kv4.2 subunits in each I_{SA} channel complex.

EXPERIMENTAL PROCEDURES

Molecular Biology—Human charybdotoxin-sensitive Kv4.2 (15, 16), KChIP2 (accession number AF199598), and DPP6-s (previously DPPX and DPL-1, accession number NP_001927) were expressed in pRAT, a dual purpose vector, for expression in mammalian cells and *in vitro* transcription. C-terminal 1d4-tagged Kv4.2 was used for both electrophysiological and biochemical studies, as previously reported (15, 16). For biochemical studies, a linker and hemagglutinin (HA) epitope were introduced at the C terminus of DPP6 using PCR with a primer for the protein sequence (TRYPYDVPDYA).

To create the tandem, Kv4.2-Kv4.2 (KK), an AscI site was introduced into the twelfth residue, and a MluI site was introduced before the termination codon of Kv4.2. Subsequently, a Kv4.2 fragment was released by digestion with AscI and MluI and inserted into a Kv4.2-containing plasmid opened by MluI; the last residue of the first Kv4.2 subunit is thus linked to the twelfth residue of the second Kv4.2 subunit by an additional arginine residue. To produce Kv4.2-DPP6 (KD) and Kv4.2-Kv4.2-DPP6 (KKD) constructs, an AscI site was introduced into the second residue, and a MluI site was introduced before the termination codon of DPP6. A fragment of DPP6 was released with AscI and MluI and inserted into Kv4.2 or KK containing plasmid opened by MluI. Correct orientation of the insert was confirmed by enzyme digestion and DNA sequencing. cRNA was synthesized after linearization with NotI using the T7 promoter and mMessage mMachine kit (Ambion, Austin, TX) and quantified by spectroscopy.

Electrophysiology and Data Analysis—Oocytes from *Xenopus laevis* were defolliculated with collagenase and microinjected with 0.05–0.50 ng of a mixture of pore former and DPP6 subunit cRNAs at 1:2 molar ratio, a ratio chosen to reproducibly recapitulate the effects of DPP6 on Kv4.2 (4) studied 18–48 h

* This work was supported, in whole or in part, by National Institutes of Health Grant GM051851. The costs of publication of this article were defrayed in part by the payment of page charges. This article must therefore be hereby marked "*advertisement*" in accordance with 18 U.S.C. Section 1734 solely to indicate this fact.

[1] Supported by Korea Research Foundation Grant KRF-2003-037-C00100.

[2] To whom correspondence should be addressed: Dept. of Pediatrics and Institute for Molecular Pediatric Sciences, Pritzker School of Medicine, Biological Sciences Division, University of Chicago, 5721 S. Maryland Ave., Chicago, IL 60637. E-mail: sangoldstein@uchicago.edu.

[3] The abbreviations used are: DPP, dipeptidyl aminopeptidase; HA, hemagglutinin; D, DPP6; K, Kv4.2; KD, Kv4.2-DPP6; KK, Kv4.2-Kv4.2; KKD, Kv4.2-Kv4.2-DPP6; DTBP, dimethyl 3,3′-dithiobispropionimidate; CHAPS, 3-[(3-cholamidopropyl)dimethylammonio]-1-propanesulfonic acid.

post-injection. Whole cell currents were measured by two-electrode voltage-clamp (oocyte clamp OC-725A; Warner Instruments, Hamden, CT). The electrodes were filled with 3 M KCl and had resistances of 0.1–0.6 MΩ. The data were sampled at 1 kHz. Data recording was performed using Clampex v8.0 and assessed with Clampfit v9.0 (Molecular Devices, Inc.), Excel (Microsoft, Inc.) and Origin ver6.1 (Rockware, Inc.). All of the experiments were performed at room temperature. The standard bath solution was ND-96 (96 mM NaCl, 2 mM KCl, 1 mM $MgCl_2$, 1.8 mM $CaCl_2$, 5 mM HEPES-NaOH, pH 7.5). The voltage families were obtained from a holding potential of −110 mV with test steps from −80 to +60 mV for 250 ms with 10-mV increments every 10 s; subtraction of currents recorded at test potentials following a 1-s prepulse to −40 mV like others (17) or P/4 protocols were employed. Steady state inactivation was examined from a holding potential of −100 mV with test pulses from −110 to −20 mV held for 2.5 s with a second pulse to 40 mV to measure currents that were not inactivated. $V_{0.5}$ of activation and $V_{0.5}$ of steady state inactivation were calculated by fitting the normalized conductance-voltage relationships with a Boltzmann function (18). Recovery from inactivation was measured by driving channels to an inactivated state at +40 mV, hyperpolarizing to −110 mV, and then applying a second pulse to +40 mV for various intervals (increments of 10 or 25 ms). Inactivation was fitted with a double exponential equation and recovery from inactivation with a single exponential equation. One way analysis of variance was used for statistical tests using Origin ver6.1 software.

Expression in COS7 Cells and Purification and Amino Acid Analysis—COS7 cells were transfected with 5 μg of Kv4.2, 10 μg of DPP6, and 10 μg of KChIP2 cDNA/150-mm plate using Lipofectamine 2000 (Invitrogen). Two days after transfection, the cells were incubated in cross-linking buffer containing 150 mM KCl, 50 mM HEPES, pH 7.4, and 1 mg/ml dimethyl 3,3′-dithiobispropionimidate (DTBP; Pierce) for 1 h at room temperature to preserve protein-protein interactions between Kv4.2 and DPP6 (4). The cells from 10–20 plates were solubilized for 1 h at 4 °C in lysis buffer containing 2.5% CHAPS, 100 mM NaCl, 40 mM KCl, 1 mM EDTA, 20 mM HEPES-KOH, pH 7.4, and 10% glycerol with complete protease inhibitors (Roche Applied Science). Soluble material was collected after centrifugation at 100,000 × *g* for 45 min. The extract was incubated with an anti-1d4 antibody immobilized on Sepharose beads (19) for 1 h at 4 °C with agitation. The beads were washed with 100 ml of wash buffer containing 0.7% CHAPS, 300 mM NaCl, 40 mM KCl, 1 mM EDTA, 20 mM HEPES-KOH, pH 7.4. Protein was then eluted with 0.7% CHAPS, 100 mM NaCl, 40 mM KCl, 1 mM EDTA, 20 mM HEPES-KOH, pH 7.4, complete protease inhibitor, and 0.1 mg/ml 1d4 peptide (Yale University Keck Facility, New Haven, CT). Finally, cross-links were cleaved by reduction with 2.5% 2-mercaptoethanol in SDS-PAGE sample loading buffer for 30 min at room temperature. Mouse anti-1d4 (NCCC, Minneapolis, MN) and rat anti-HA (Roche Applied Science) monoclonal antibodies were purchased, and KChIP2 antibodies were a generous gift (J. Trimmer, University of California, Davis). After SDS-PAGE and staining with Coomassie Brilliant Blue, bands corresponding to Kv4.2, DPP6, and a blank portion of the gel were excised with a sterile scalpel. The samples were hydrolyzed, and the amino acids were quantified (Yale University Keck Facility). Amino acids determined for the blank gel sample were subtracted from test samples to correct for background. These methods have previously been described in detail (15).

RESULTS

DPP6 Impacts Current Magnitude in Channels with Fixed Subunit Ratios—A canonical effect of DPP6 is an increase current density (4). Thus, natural assembly of DPP6 (D) and Kv4.2 (K) subunits in *Xenopus* oocytes produced a significant increase in current when assessed by two electrode voltage clamp (Fig. 1*A*); augmentation led to ~10-fold greater current than with K subunits alone (Fig. 1*B*). To assess the number of D subunits required in each channel to enhance K currents, fusion proteins were created to enforce subunit ratios. This was accomplished via synthesis of genes encoding proteins linking two K subunits (KK), two K with one D (KKD), and one K with one D (KD). Because D has an intracellular N terminus, it was fused to the cytoplasmic C terminus of Kv4.2.

KKD proteins enforce a subunit ratio of 2:1 and were designed to yield channels with four K subunits and two D (Fig. 1*A*); although KKD channels were active, their current magnitudes were small like channels formed only with Kv4.2 subunits. Conversely, KD proteins with a 1:1 subunit ratio (designed to incorporate four D subunits per channel) showed an ~5-fold augmentation in currents compared with KKD channels. Supporting the idea that channels formed by KKD required additional D subunits, co-expression of monomer D with K, KK, and KKD subunits resulted in an ~10-fold increase in current amplitude (Fig. 1*B*); conversely, KD current levels were less sensitive to free D, increasing just 3-fold. Although any effect of D on KD channels raised concern that more than four D subunits were required in each channel, gating and protein composition studies suggested otherwise.

KD Channels Operate Like Those Naturally Formed of Kv4.2 and DPP6 Subunits—Studies of gating kinetics indicated a 4:4 ratio of K:D subunits was required and sufficient to yield the biophysical characteristics of naturally assembled channels (Table 1). Further, the characteristics of KD channels were not significantly altered by additional D subunits, suggesting that they were complete (Table 1).

To display the effects of D on the various linked pore-forming subunits, representative current traces in the absence and presence of monomer D at 0 mV were normalized to peak current and overlaid for comparison (Fig. 2). Assembly with monomer D sped activation and inactivation of K as expected (Fig. 2*A*) and impacted KK and KKD similarly (Fig. 2, *B* and *C*). Conversely, monomer D had no effect on KD channel gating (Fig. 2*D*), and kinetics of activation and inactivation of KD channels were similar to channels formed naturally by K + D subunits (Fig. 2*E*).

These impressions gleaned by visual inspection were supported by the determined gating parameters (Fig. 3 and Table 1). Thus, monomer D produced a 20-mV hyperpolarizing shift in the voltage dependence of half-maximal activation of K channels ($V_{0.5}$ = ~−23 mV) compared with those assembled of K + D subunits ($V_{0.5}$ = ~−43 mV; Fig. 3*A*, *top panel*, and Table

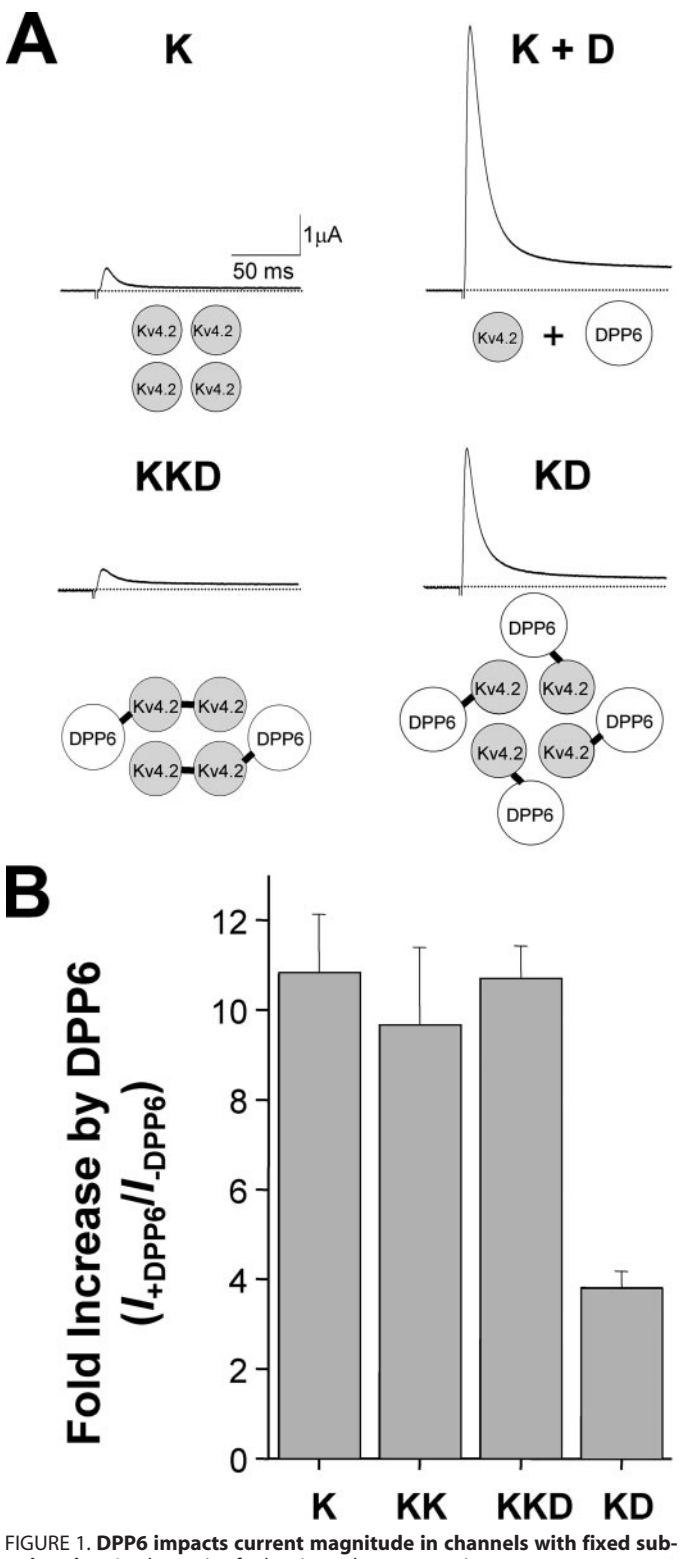

FIGURE 1. **DPP6 impacts current magnitude in channels with fixed subunit ratios.** *A*, schematic of subunits and representative current traces at +40 mV for channels assembled with K and D or the linked subunits KKD and KD measured in *Xenopus* oocytes by two-electrode voltage clamp. *B*, relative peak current density at +40 mV for various pore-forming subunits in the absence and presence of D. These were calculated from three to six different groups of oocytes, each group with 5–16 cells. The raw currents from one group (μA mean ± S.E.) at +40 mV with indicated subunits were: K, 0.64 ± 0.15 (n = 10); K + D, 8.28 ± 0.5 (n = 6); KK, 0.64 ± 0.09 (n = 8); KK + D, 6.26 ± 0.46 (n = 9); KKD, 0.78 ± 0.05 (n = 7); KKD + D, 8.23 ± 0.81 (n = 8); KD, 3.4 ± 0.2 (n = 9); KD + D, 10.2 ± 0.4 (n = 7).

1. Whereas linkage-enforced 1:1 association in KD channels also led to a 20-mV shift ($V_{0.5}$ = ~−45 mV), KKD channels showed only an intermediate shift to $V_{0.5}$ = ~−35 mV (significantly different from KD) unless assembled with monomer D ($V_{0.5}$ = ~−45 mV) (Fig. 3, *A* and *B*, *top panels*, and Table 1).

Similarly, comparison of K and K + D channels revealed D to produce a hyperpolarizing shift in the voltage dependence of steady state inactivation (from $V_{0.5}$ = ~−58 mV to −71 mV) that was recapitulated by linkage-enforced 1:1 subunit association to yield KD channels ($V_{0.5}$ = ~−72 mV). In contrast, KKD channels shifted to an intermediate level significantly different from KD ($V_{0.5}$ = ~−64 mV) unless assembled with additional monomer D ($V_{0.5}$ = ~−72 mV) (Fig. 3, *A* and *B*, *middle panels*, and Table 1). Moreover, the kinetic components of inactivation (fast τ, slow τ, and their weighting) modified by assembly of K with D were recapitulated in KD channels and not KKD channels (Table 1).

Further, speeding of time to peak by monomer D (from 33 ms at −30 mV for K channels to 12 ms for those assembled with D subunits) was recapitulated in KD channels, whereas KKD channels showed an intermediate time course that was enhanced on assembly with additional monomer D (Fig. 3, *A* and *B*, *middle panels*, and Table 1). All of these findings were consistent with a 4:4 subunit ratio in naturally assembled channels.

A 4:4 subunit ratio was not implied by the observation that both KD and KKD channels had rapid rates of recovery from inactivation as if just two D subunits were sufficient to produce this behavior (Table 1). Further, KKD channels assembled with monomer D failed to inactivate like K + D channels, revealing that KKD subunits did not fully recapitulate the attributes of channels formed solely with monomer subunits.

KChIP2 Does Not Alter Stoichiometry Inferred by Function—The ratio of K and D subunits in naturally assembled channels appeared to be preserved in the presence of KChIP2. KChIP2 assembles with Kv4 subunits with a 4:4 ratio to produce cardiac I_{to} currents (15, 16, 20, 21). Jerng *et al.* (6) suggest that neuronal I_{SA} channels include Kv4 and DPP6 (and/or DPP10) as well as KChIPs based on their co-purification. The effects of D were therefore studied with added KChIP2.

KChIP2 induces a hyperpolarizing shift in the voltage dependence of activation of Kv4.2 channels (although less than DPP6) and a small depolarizing shift in the voltage dependence of steady state inactivation (15). KChIP2 and D assembled with K, KK, or KKD subunits decreased the hyperpolarizing shift in voltage-dependent activation and steady state inactivation in all cases by ~50% while leaving accelerated time to peak unaltered (Table 1). Further, KD and K + D channels showed the same gating parameters with KChIP2 (Table 1), whereas there was a significant difference between the time to peak of KD + KChIP2 (~13 ms) and KKD + KChIP2 (~20 ms) channels.

Amino Acid Analysis of Naturally Assembled Channels—Because KChIP2 increased the solubility (22) and yield (15) of Kv4 channels and did not appear to alter the stoichiometry of K + D channels, naturally assembled channels were expressed with KChIP2 for amino acid analysis. Purification was achieved via antibodies to an epitope tag encoded on the Kv4.2 C terminus

TABLE 1

Channel gating parameters for various Kv4.2 channel complexes

Voltage clamp was performed as described under "Experimental Procedures" (number of oocytes). One-way analysis of variance was used for statistical tests using Origin ver6.1.

Channel subunits expressed	Activation $V_{0.5}$	Inactivation $V_{0.5}$	Time to peak at −30 mV	Inactivation			Recovery from inactivation at +40 mV
				Fast	Slow	$A_{fast}/(A_{fast} + A_{slow})$	
	mV	*mV*	*ms*	*ms*	*ms*		*ms*
Monomer							
K	−22.5 ± 1.7 (5)	−57.6 ± 1.5 (7)	32.8 ± 1.8 (6)	18.6 ± 0.9 (9)	199 ± 31 (9)	0.83 ± 0.01 (9)	139.8 ± 9.4 (7)
K + D	−43.1 ± 0.9 (8)	−71.1 ± 1.3 (8)	11.5 ± 0.4 (8)	13.4 ± 0.8 (10)[c]	145 ± 35 (10)	0.95 ± 0.01 (10)[c]	40.2 ± 3.3 (6)
K + D + KChIP2	−34.4 ± 1.7 (7)	−55.7 ± 0.9 (7)	12.1 ± 0.8 (7)	ND	ND	ND	12.5 ± 0.8 (7)
Linked							
KD	−44.8 ± 1.1 (8)	−72.0 ± 0.9 (8)	12.1 ± 0.5 (7)	11.8 ± 0.4 (6)	127 ± 15 (6)	0.92 ± 0.01 (6)	43.9 ± 1.8 (6)
KD + KChIP2	−33.0 ± 1.9 (7)	−57.7 ± 1.1 (7)	13.0 ± 0.8 (7)	ND	ND	ND	8.8 ± 0.6 (4)
KKD	−34.5 ± 1.0 (7)[a]	−64.3 ± 1.0 (9)[a]	18.0 ± 0.6 (8)[a]	21.9 ± 1.8 (9)	186 ± 38 (9)	0.69 ± 0.02 (9)	50.9 ± 5.9 (6)
KKD + KChIP2	−29.4 ± 1.6 (7)	−54.6 ± 0.8 (7)	21.3 ± 2.0 (6)[b]	ND	ND	ND	9.7 ± 1.0 (4)
Controls							
KK	−21.6 ± 1.8 (7)	−56.3 ± 1.8 (8)	38.1 ± 2.5 (8)	24.2 ± 2.1 (6)	252 ± 55 (6)	0.71 ± 0.02 (6)	154.1 ± 7.6 (6)
KK + D	−45.1 ± 1.0 (7)	−69.6 ± 1.0 (7)	10.6 ± 0.5 (7)	15.5 ± 1.2 (7)[c]	235 ± 51 (7)	0.86 ± 0.02 (7)[c]	45.4 ± 3.0 (6)
KD + D	−47.9 ± 0.7 (4)	−75.9 ± 0.5 (4)	9.5 ± 0.2 (5)	11.7 ± 0.3 (7)	158 ± 24 (7)	0.93 ± 0.01 (7)	ND
KKD + D	−46.1 ± 2.1 (5)	−71.9 ± 0.7 (5)	10.1 ± 0.5 (5)	19.1 ± 0.6 (5)	124 ± 19 (5)	0.79 ± 0.01 (5)[c]	ND
KK + D + KChIP2	−34.2 ± 1.8 (7)	−55.7 ± 0.9 (5)	12.8 ± 0.5 (7)	ND	ND	ND	13.6 ± 1.4 (6)

[a] Difference significant ($p = 0.001$) compared with K + D.
[b] Difference significant ($p = 0.005$) compared with K + D + KChIP2.
[c] Difference significant ($p = 0.005$) compared with no monomer DPP6.

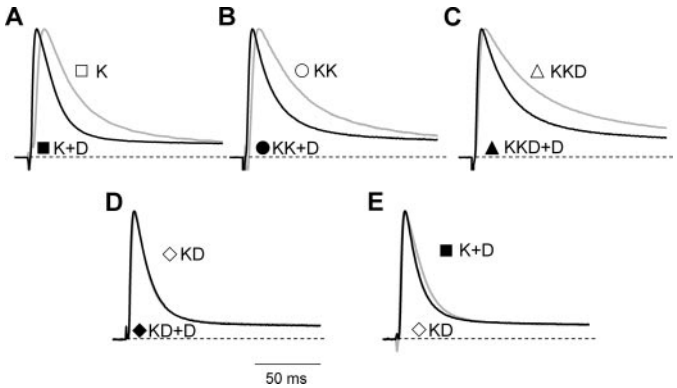

FIGURE 2. **Natural and KD channels show similar kinetic properties.** Normalized and superimposed representative current traces at 0 mV for channels with D (*filled symbols*, *dark lines*) or without D (*open symbols*, *gray lines*) and the pore-forming subunits K, KK, KD, and KKD. *A*, K *versus* K + D. *B*, KK *versus* KK + D. *C*, KKD *versus* KKD + D. *D*, KD *versus* KD + D. *E*, overlay of KD and K + D; inactivation fast component for traces shown: K + D and KD, τ_{fast} = 13.4 and 11.8 ms, respectively.

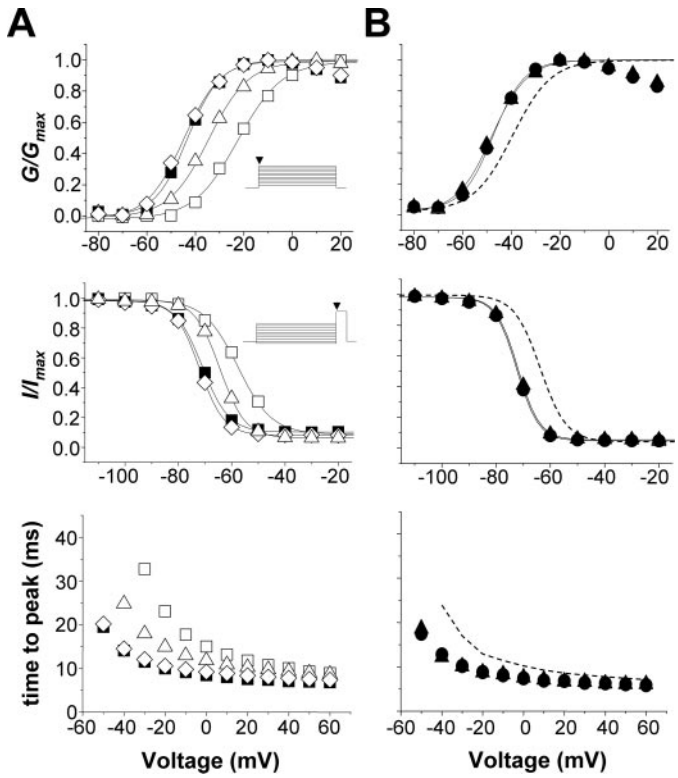

FIGURE 3. **Biophysical properties of natural and engineered channels.** *A*, conductance-voltage relationships, steady state inactivation-voltage relationships, and time to peak for K (*open square*), KKD (*open triangle*), KD (*open diamond*), and K + D (*filled square*) for biophysical parameters listed in Table 1. The *insets* show voltage protocol as described under "Experimental Procedures" with *arrowheads* to indicate where current was measured. *B*, assembly with monomer D (*filled symbols*) shifts KKD channel (*triangle*) G-V and steady state inactivation-voltage relationships and time to peak (*dashed line* from data in *A*) to those measured for natural K + D (*square*) and KD (*diamond*) channels. The biophysical parameters are listed in Table 1.

(Fig. 4). Thus, K, D, and KChIP2 were transiently expressed in COS7 cells, channels in the plasma membrane were cross-linked with DTBP, and immunopurification was achieved after detergent solubilization. SDS-PAGE and Western blot analysis confirmed co-purification of the three subunit types (Fig. 4*A*). Ready staining with Coomassie Brilliant Blue confirmed the channel complex to be rich in the channel subunits (Fig. 4*B*).

Other proteins that co-purified were identified by mass spectrometry to be a heat shock protein, tubulin, trypsin precursor, and actin (Fig. 4). To accurately assess the relative amounts of K and D subunits, the bands visualized by staining with dye were excised from the gel for amino acid analysis by hydrolysis, ion exchange chromatography, and ninhydrin detection (Table 2). Because the sequences of the subunits were known, expected and observed amino acid content of the bands were used to calculate the moles of each subunit from analysis of five to nine residues in five independent trials. The ratio of K:D in purified complexes was 1.1 ± 0.3 (Table 2), indicative of a 1:1 molar ratio and thus four K and four D subunits in each channel. In agreement with previous findings (4, 6), we observed the association of K and D subunits to be better preserved in the presence of the

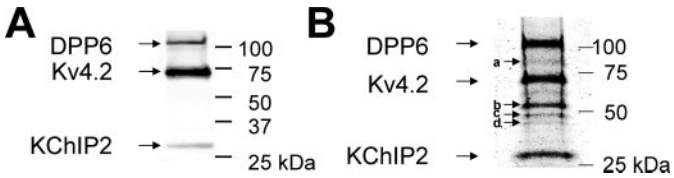

FIGURE 4. **Amino acid analysis of naturally assembled channels.** Purification of channels formed in COS7 cells with K, D, and KChIP2 subunits was achieved via a 1d4 epitope on K after treatment with DTBP. Purified proteins were subjected to reducing conditions to reverse DTBP linkages and separated by SDS-PAGE. *A*, proteins detected by Western blotting with anti-1d4 (Kv4.2–1d4), anti-HA (DPP6-HA), and anti-KChIP2 monoclonal antibodies. *B*, proteins detected with Coomassie Brilliant Blue. Bands corresponding to K and D were excised and subjected to amino acid analysis (Table 2). *Bands a*, *b*, *c*, and *d* co-purified and were identified by mass spectrometry to be a 90-kDa heat shock protein, a tubulin, a trypsin precursor, and an actin, respectively (data not shown).

TABLE 2

Molar ratio of DPP6 and Kv4.2 subunits

Individual amino acids used to quantify yield were within 10% of predicted. The ratios indicate mol of Kv4.2:DPP6.

Experiment	Kv4.2	DPP6	Ratio
	Pmol	*Pmol*	
1	8.4	6.2	0.74
2	17.4	18.7	1.07
3	3.8	5.8	1.53
4	3.4	3.2	0.94
5	8.2	7.9	0.96

chemical cross-linking agent, DTBP. Approximately half as much D protein was recovered on purification of complexes in the absence of cross-linker (Kv4.2:DPP6, 0.44 ± 0.06, $n = 5$).

DISCUSSION

Auxiliary subunits are an important feature in potassium channel physiology because they influence channel location, abundance, sensitivity to stimulation, and pharmacology *in vivo* (22–24). Here, we show that D and K subunits assemble naturally with a stoichiometry of 4:4. Previous studies demonstrated that D increases K channel trafficking to the plasma membrane, produces a hyperpolarizing shift in both the conductance-voltage relationship and steady state inactivation, decreases time to peak, accelerates inactivation kinetics, and increases the rate of recovery from inactivation (4). These modulatory effects were used here to deduce the stoichiometry of channel complexes by comparing naturally assembled and engineered constructs linking K and D proteins. Thereafter, direct amino acid analysis was performed to support the inferred subunit ratio.

Whereas linked KD subunits enforcing a 1:1 subunit ratio generated channel complexes that showed biophysical characteristics comparable with those of channels formed naturally, KKD subunits did not do so without additional D monomers. Four D subunits per channel were required to reproduce natural voltage-dependent activation, voltage-dependent steady state inactivation, and time to peak, whereas two were sufficient to replicate recovery from inactivation. Arguing for the trustworthiness of linked subunits in this analysis, the same effects were observed on assembly of D with K or KK subunits (Table 1). Moreover, linkage to produce KK channels did not alter the conductance-voltage relationship, steady state inactivation voltage relationship, time to peak, nor rate of recovery from inactivation relative to K channels (Table 1). KK channels did inactivate more slowly than K channels. This was likely due to linkage of the N and C termini because deletion studies have suggested that both termini in Kv4.1 are required to confer rapid inactivation (25). A similar rationale may explain small differences in inactivation rates of K + D and KD channels (Fig. 2*E* and Table 1).

Direct biochemical analysis also supported 4:4 stoichiometry. In agreement with others (4, 6), we recovered more D via K isolation when cells were treated with a cross-linking agent prior to detergent solubilization. Although use of a cross-linker should arouse suspicion, studies of intact cells showed no requirement for chemical stabilization to observe similar attributes for K + D and KD channels (Table 1). This suggests that D subunit association is not dynamic or variable for channels in the plasma membrane.

Disruption of membrane complexes on detergent solubilization can simply reflect destabilization in the absence of an enveloping membrane; conversely, it suggests consideration of a model with D in a lipid-exposed, peripheral location given that the single-span accessory subunit MinK is detergent-stable in complexes with KCNQ1 (13) and thought to be deeply intercalated/pore-associated (26, 27). Further, the observation that KD channel surface delivery is enhanced by expression with added monomer D (Fig. 1*B*) leaves open the possibility that more than four DPP6 subunits are associated during intracellular channel trafficking.

Although the extracellular domain of DPP6 has been crystallized and its structure has been solved (28), it remains to be determined how the single transmembrane domain of D is incorporated within the channel complex. Studies of DPP6 and DPP10 suggest that the transmembrane domain is important in the association with Kv4 channels (7, 29). Indeed, DPP6 destabilized resting and intermediate states in the voltage-dependent activation pathway negatively shifting the gating charge-voltage relationship apparently via interaction of the transmembrane domain and Kv voltage-sensing and pore domains (30). Another report argues for direct contact of the DPP10 transmembrane domain and S1 and/or S2 transmembrane domains of Kv4.3 subunits (29).

Jerng *et al.* (6) have suggested that neuronal I_{SA} channels include Kv4, DPP6 (and/or DPP10), and KChIPs. In support of these findings, we also observed co-purification of the three subunit types and faster recovery from inactivation with both KChIP2 and DPP6 compared with channels with either accessory subunit alone (Table 1). Jerng *et al.* (6) also report inactivation of K4.2-DPP10-KChIP3 channels to be faster than Kv4.2-DPP6-KChIP3 channels, suggesting that different subunit combinations may produce functional diversity in neurons. We expected to demonstrate a 1:1:1 ratio for K:D:KChIP subunits because K:KChIP channels show a 1:1 ratio in biochemical (15), electron microscopic (16), and x-ray crystallographic studies (20). However, KChIP recovery on expression with K and D was twice the level expected in both the absence and presence of cross-linker (2.17 ± 0.16 and 2.05 ± 0.18, respectively, $n = 4–7$). We suspect this to be an artifact of the method but cannot rule out the possibility that D increases the number of KChIP subunits in channel complexes.

Recovery of tubulin, actin, and heat shock protein with Kv4.2, DPP6, and KChIP2 was not unexpected. The cytoskeletal proteins have previously been isolated with Kv4 (31), Kv1.5 (32), Kir2.1 (33) and chloride channels (34) and heat shock proteins with HERG (35) and chloride channels (36).

Only two MinK subunits assemble with four KCNQ1 pore-forming subunits to form cardiac I_{Ks} potassium channels (13, 14, 37). In contrast, voltage- and calcium-activated BK potassium channels (38, 39) and Kir6.2 potassium channels (40, 41) are thought to employ four transmembrane auxiliary subunits and four pore-forming subunits, as observed here for D and K. A subunit stoichiometry of 4:4 has also been reported for two soluble intracellular regulators of potassium channels, KChIP with Kv4 (16, 20, 21) and Kvβ2 with Kv1.1 (42).

It should be noted, however, that variability of BK channel behavior *in vivo* has been hypothesized to reflect assemblies with less than four auxiliary subunits based on studies of mammalian subunits expressed in *Xenopus* oocytes (43). Our data do not rule out the possibility that channels with fewer than four D may form in native cells, for example, should D and K subunits be down-regulated asynchronously. However, the major mechanism by which DPP subunits augment Kv4.2 current is to increase surface delivery of channels (5, 7) and both K and KKD subunits produced small currents unless assembled with monomer D (Fig. 1). It seems likely, therefore, that 4:4 complexes predominate on the surface of cells producing D and K subunits and that a 4:4 arrangement is the norm for DPP subunits in assemblies with Kv pore-forming partners.

Acknowledgments—We thank K. Wada for the DPP6 plasmid and J. Trimmer (University of California, Davis) for anti-KChIP2 antibodies. We thank D. Goldstein, A. Kollewe, A. Lewis, L. Plant, Z. McCrossan, and Y. Mishina for help during the performance of the studies and critical feedback on the manuscript.

REFERENCES

1. Johns, D. C., Nuss, H. B., and Marban, E. (1997) *J. Biol. Chem.* **272,** 31598–31603
2. Liss, B., Franz, O., Sewing, S., Bruns, R., Neuhoff, H., and Roeper, J. (2001) *EMBO J.* **20,** 5715–5724
3. Malin, S. A., and Nerbonne, J. M. (2000) *J. Neurosci.* **20,** 5191–5199
4. Nadal, M. S., Ozaita, A., Amarillo, Y., de Miera, E. V.-S., Ma, Y., Mo, W., Goldberg, E. M., Misumi, Y., Ikehara, Y., Neubert, T. A., and Rudy, B. (2003) *Neuron* **37,** 449–461
5. Jerng, H. H., Qian, Y., and Pfaffinger, P. J. (2004) *Biophys. J.* **87,** 2380–2396
6. Jerng, H. H., Kunjilwar, K., and Pfaffinger, P. J. (2005) *J. Physiol. (Lond.)* **568,** 767–788
7. Zagha, E., Ozaita, A., Chang, S. Y., Nadal, M. S., Lin, U., Saganich, M. J., McCormack, T., Akinsanya, K. O., Qi, S. Y., and Rudy, B. (2005) *J. Biol. Chem.* **280,** 18853–18861
8. An, W. F., Bowlby, M. R., Bett, M., Cao, J., Ling, H. P., Mendoza, G., Hinson, J. W., Mattsson, K. I., Strassle, B. W., Trimmer, J. S., and Rhodes, K. J. (2000) *Nature* **403,** 553–556
9. Dixon, J. E., Shi, W. M., Wang, H. S., McDonald, C., Yu, H., Wymore, R. S., Cohen, I. S., and McKinnon, D. (1996) *Circ. Res.* **79,** 659–668
10. Fiset, C., Clark, R. B., Shimoni, Y., and Giles, W. R. (1997) *J. Physiol.* (*Lond.*) **500,** 51–64
11. Kaab, S., Dixon, J., Duc, J., Ashen, D., Nabauer, M., Beuckelmann, D. J., Steinbeck, G., McKinnon, D., and Tomaselli, G. F. (1998) *Circulation* **98,** 1383–1393
12. Brahmajothi, M. V., Campbell, D. L., Rasmusson, R. L., Morales, M. J., Trimmer, J. S., Nerbonne, J. M., and Strauss, H. C. (1999) *J. Gen. Physiol.* **113,** 581–600
13. Chen, H., Kim, L. A., Rajan, S., Xu, S., and Goldstein, S. A. N. (2003) *Neuron* **40,** 15–23
14. Wang, K. W., and Goldstein, S. A. N. (1995) *Neuron* **14,** 1303–1309
15. Kim, L. A., Furst, J., Butler, M. H., Xu, S., Grigorieff, N., and Goldstein, S. A. (2004) *J. Biol. Chem.* **279,** 5549–5554
16. Kim, L. A., Furst, J., Gutierrez, D., Butler, M. H., Xu, S., Goldstein, S. A., and Grigorieff, N. (2004) *Neuron* **41,** 513–519
17. Nadal, M. S., Amarillo, Y., Vega-Saenz de Miera, E., and Rudy, B. (2001) *J. Physiol.* **537,** 801–809
18. Clay, J. R. (2000) *Eur. Biophys. J.* **29,** 555–557
19. Sokolova, O., Kolmakova-Partensky, L., and Grigorieff, N. (2001) *Structure* **9,** 215–220
20. Pioletti, M., Findeisen, F., Hura, G. L., and Minor, D. L. (2006) *Nat. Struct. Mol. Biol.* **13,** 987–995
21. Wang, H., Yan, Y., Liu, Q., Huang, Y., Shen, Y., Chen, L., Chen, Y., Yang, Q., Hao, Q., Wang, K., and Chai, J. (2007) *Nat. Neurosci.* **10,** 32–39
22. Shibata, R., Misonou, H., Campomanes, C. R., Anderson, A. E., Schrader, L. A., Doliveira, L. C., Carroll, K. I., Sweatt, J. D., Rhodes, K. J., and Trimmer, J. S. (2003) *J. Biol. Chem.* **278,** 36445–36454
23. Abbott, G. W., and Goldstein, S. A. N. (1998) *Q. Rev. Biophys.* **31,** 357–398
24. Rhodes, K. J., Strassle, B. W., Monaghan, M. M., Bekele-Arcuri, Z., Matos, M. F., and Trimmer, J. S. (1997) *J. Neurosci.* **17,** 8246–8258
25. Jerng, H. H., and Covarrubias, M. (1997) *Biophys. J.* **72,** 163–174
26. Tai, K. K., and Goldstein, S. A. N. (1998) *Nature* **391,** 605–608
27. Melman, Y. F., Um, S. Y., Krumerman, A., Kagan, A., and McDonald, T. V. (2004) *Neuron* **42,** 927–937
28. Strop, P., Bankovich, A. J., Hansen, K. C., Christopher Garcia, K., and Brunger, A. T. (2004) *J. Mol. Biol.* **343,** 1055–1065
29. Ren, X., Hayashi, Y., Yoshimura, N., and Takimoto, K. (2005) *Molecular and Cellular Neuroscience* **29,** 320–332
30. Dougherty, K., and Covarrubias, M. (2006) *J. Gen. Physiol.* **128,** 745–753
31. Petrecca, K., Miller, D. M., and Shrier, A. (2000) *J. Neurosci.* **20,** 8736–8744
32. Mason, H. S., Latten, M. J., Godoy, L. D., Horowitz, B., and Kenyon, J. L. (2002) *Mol. Pharmacol.* **61,** 285–293
33. Sampson, L. J., Leyland, M. L., and Dart, C. (2003) *J. Biol. Chem.* **278,** 41988–41997
34. Jentsch, T. J., Stein, V., Weinreich, F., and Zdebik, A. A. (2002) *Physiol. Rev.* **82,** 503–568
35. Ficker, E., Dennis, A. T., Wang, L., and Brown, A. M. (2003) *Circ. Res.* **92,** e87–e100
36. Hinzpeter, A., Lipecka, J., Brouillard, F., Baudoin-Legros, M., Dadlez, M., Edelman, A., and Fritsch, J. (2006) *Am. J. Physiol.* **290,** C45–C56
37. Morin, T. J., and Kobertz, W. R. (2008) *Proc. Natl. Acad. Sci. U. S. A.* **105,** 1479–1482
38. Knaus, H. G., Folander, K., Garcia, C. M., Garcia, M. L., Kaczorowski, G. J., Smith, M., and Swanson, R. (1994) *J. Biol. Chem.* **269,** 17274–17278
39. Ding, J. P., Li, Z. W., and Lingle, C. J. (1998) *Biophys. J.* **74,** 268–289
40. Shyng, S., and Nichols, C. G. (1997) *J. Gen. Physiol.* **110,** 655–664
41. Clement, J. P. t., Kunjilwar, K., Gonzalez, G., Schwanstecher, M., Panten, U., Aguilar-Bryan, L., and Bryan, J. (1997) *Neuron* **18,** 827–838
42. Gulbis, J. M., Zhou, M., Mann, S., and MacKinnon, R. (2000) *Science* **289,** 123–127
43. Wang, Y.-W., Ding, J. P., Xia, X.-M., and Lingle, C. J. (2002) *J. Neurosci.* **22,** 1550–1561